International Journal of Bridge Engineering (IJBE), Vol. 9, No. 2, (2021), pp. 33-50

# NATURAL FREQUENCY OF FUNCTIONALLY GRADED DECKS PLATES WITH POROSITY BASED ON HIGHER-ORDER PLATES THEORY

Merdaci Slimane[1], Osama Mohammed Elmardi Suleiman Khayal[2] and Hadj Mostefa Adda[3]

[1] University of Djillali Liabès of Sidi Bel Abbes, Department of Civil Engineering and Public Works, Algeria
[2] Nile Valley University, Department of Mechanical Engineering, Sudan
[3] University of Rélizane, Institute of Science & Technology, Dept. of Civil Engineering, Algeria.
e-mail: slimanem2016@gmail.com, osamamm64@gmail.com

**ABSTRACT:** In this paper, free vibrations of Functionally Graded decks Plates (FGP) with two distribution even and uneven of porosity are investigated. The plate is modeled using higher-order shears deformation plate theory. It has been observed that during the manufacture of (FGP), micro-voids and porosities can occur inside the material. In the resolution and the determination of the equations of motion Hamilton principle is used. Since the deck plate is simply supported the Navier procedure will be retained. Thus, in this work, the investigation of the free vibration analysis of (FGP) deck plate taking into account the perfect and influence of these imperfect is established. Natural frequencies are obtained for porous (FGP) with edges simply supported and verified with the results shown in the literature. A numerical study is conducted to examine the effects of various parameters such as material properties, thickness ratios, geometric ratio and the porosity coefficient on natural frequencies of the (FGP). It is found that the effects of exponent graded and the porosity coefficient on the natural frequencies are significant.

**KEYWORDS:** FGP, Decks Plates, Natural Frequency, Free Vibration, HSPT, Even Porosity, Uneven Porosity.

## 1 INTRODUCTION

Functionally graded material (FGM) is a new class of composite materials whose microstructure and composition vary gradually and continuously with position so as to optimize the mechanical and thermal performance of the structure which they constitute. The desired functions are integrated, from the design, at the very heart of the material; this is done by choosing the appropriate material according to specific applications and environmental loads for each interface. These materials have multiple advantages with strength / weight ratios

and very high thickness / weight, which can make them attractive from the point of view of their application potential. The concept of functionally graded material was first considered in Japan in 1984 during a space plane project. The functionally graded materials (FGM) are produced by mixing two or more materials for a gradual distribution of the volume fractions of the constituents [1]. In practice, functionally graded materials (FGMs) find their applications in many fields, such as biomaterials, engineering structures, aerospace, electronics, aerospace, electronics, optics, etc. [2] – [12].

Several studies have been performed to analyze the vibration of functionally graded decks plates. The exact solutions for free and forced vibrations of simply supported functionally graded rectangular decks plates for three dimensional were presented by [13]. The free vibrations of functionally graded decks plates by using a global collocation method, the first and the third-order shear deformation plate theories were analyzed by [14]. Static deformations, free and forced vibrations of a thick rectangular functionally graded elastic plate were analyzed by using a higher order shear and normal deformable plate theory [15] – [17]. Three dimensional vibration solutions for rectangular functionally graded plates were presented in [18]. Natural frequencies and buckling stresses of decks plates made of functionally graded materials were analyzed taking into account the effects of transverse shear and normal deformations and rotatory inertia [19].

Several works and studies have been carried out to analyze the mechanical behavior of functionally graded plates with porosity and porous structures. They investigated the effect of porosity on the natural frequency of thick porous cellular plates by using Carrere unified formulation [20] and [21]. The free vibration characteristics of isotropic rigid porous rectangular decks plates under undrained condition and the effect of deformation coupling between solid and fluid on was studied by the same authors in Reference [22]. Vibration and buckling of annular sectorial porous plates under in-plane uniform compressive loading was discussed thoroughly in [23]. The investigation for the analysis of sandwich plates (FGM) with porosity using high order shear-deformation theory was presented by [24].

However, in the manufacture of (FGMs), micro-porosities or voids can occur in the materials during the sintering process. This is due to the large difference in solidification temperature among the material constituents [25]. The porosities that occur within (FGM) specimens made by a sequential multi-step infiltration technique is discussed in [26]. Therefore, it is important to take into account the effect of porosity in the design of (FGM) structures subjected to static and dynamic loads [27] – [32]. Consequently, in recent years more attention has been paid to studies of static and dynamic behavior of structures of (FGM) materials.

The present research focuses on the free vibration analysis performance of simply supported porous functionally graded plates (FGP) for different porosity

distributions based on the higher-order shear deformation plate theory (HSPT). Two types of porosity distributions, through the thickness direction of the plate, are supposed: even porosity and uneven porosity. The (FGP) plate are supposed to vary in the thickness direction according to a power law, which is modified to approach the characteristics of the materials in order to take into account the influence of the porosities. This theory allows a variation of higher order of the axial displacement through the depth of the plate.

Therefore, the factor of correction of shear is not necessary. The four unknown shear deformation theory is employed to deduce the equations of motion from Hamilton's principle. The equations of motion of the (FGP) are determined by applying Hamilton's principle and a Navier-type analytical solution. The accuracy of this theory is verified by comparing the developed results with those obtained using other plate theories. The effects of various parameters such as volume fraction and material index, porosity distribution and length /thickness ratio on natural frequencies of simply supported (FGP) are discussed.

## 2 THEORETICAL FORMULATIONS

### 2.1 Description of the model

Consider a thick rectangular deck plate (FGP) of length a, width b and thickness h made of functionally graded material together with the adopted coordinate system as shown in Figure 1. As can be observed in Figure 2(a) and Figure 2(b), the embedded (FGP) deck plate becomes an imperfect (FGP) plate due to the effect of even and uneven porosities in its material properties distribution. The material properties of the deck plate (FGP), such as Young's modulus E, is assumed to be a function of the volume fraction of constituent materials.

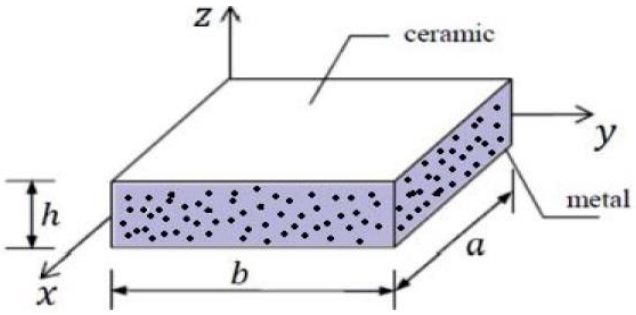


*Figure 1.* Geometric configuration of deck plate (FGP) with porosity

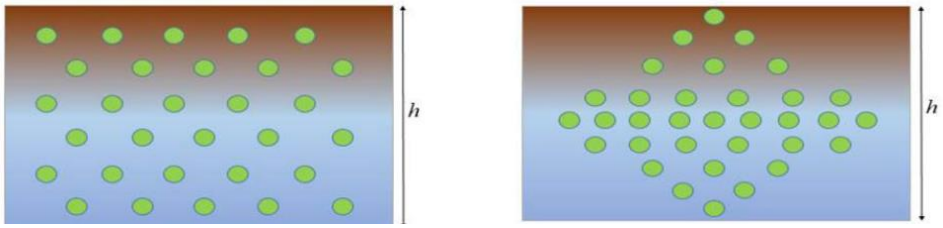


(a) Even Porosity (b) Uneven Porosity

*Figure 2.* Distributions porosity models

## 2.2 POROSITY-DEPENDENT FUNCTIONALLY GRADED MATERIALS

Assume that the (FGP) deck plate is made of a mixture of metal and ceramic. It is manifested that the material properties of the (FGP) deck plate (i.e. Young's modulus $E$, Poisson's ratio ν, and mass density $\rho$) are changed continuously with the material composition (i.e. ceramic and metal) in the thickness direction. The bottom surface of the rectangular deck plate is assumed to be metal and the top surface is made of ceramic. Furthermore, the influence of porosities, which may exist inside the materials of the (FGP) plate during the production, is included. The modified mixture rule for the two-phase (FGP) deck plate with even porosities can be expressed as follows: [30].

$$E(z) = E_m\left(1 - V - \frac{\xi}{2}\right) + E_c\left(V - \frac{\xi}{2}\right) \quad \text{And} \quad V = \left(\frac{1}{2} + \frac{z}{h}\right)^p \tag{1}$$

In which the subscripts $c$ and $m$ represent the ceramic and metal, respectively.

Also, the superscript $P$ is the volume fraction index (i.e. power-law index) that defines the material variation characterization through the thickness of the deck plate, and $\xi$ ($0 \le \xi \le 1$) shows the porosity volume fraction. $E_c$ and $E_m$ are the material properties of the ceramic and the metal, respectively.

By expanding Equation (1), the material properties of imperfect (FGP) deck plate with even porosities (i.e. the model is shown in Figure 2 (a)) can be rewritten as follow [27]:

$$E(z) = \left(E_c - E_m\right)\left(\frac{1}{2} + \frac{z}{h}\right)^p + E_m - \frac{\xi}{2}\left(E_c + E_m\right) \tag{2a}$$

$$\rho(z) = \left(\rho_c - \rho_m\right)\left(\frac{1}{2} + \frac{z}{h}\right)^p + \rho_m - \frac{\xi}{2}\left(\rho_c + \rho_m\right) \tag{2b}$$

For the second distribution model, the porosities may spread randomly through the thickness direction (i.e. known as uneven distribution) of the (FGP) deck plate (the model is shown in Figure 2 (b)) as follow [27]:

$$E(z)=\left(E_c-E_m\right)\left(\frac{1}{2}+\frac{z}{h}\right)^p+E_m-\frac{\xi}{2}\left(E_c+E_m\right)\left(1-\frac{2|z|}{h}\right) \tag{3a}$$

$$\rho(z)=\left(\rho_c-\rho_m\right)\left(\frac{1}{2}+\frac{z}{h}\right)^p+\rho_m-\frac{\xi}{2}\left(\rho_c+\rho_m\right)\left(1-\frac{2|z|}{h}\right) \tag{3b}$$

## 3 KINEMATICS AND STRAINS RELATIONS

Based on the assumptions made in the previous section, the displacements fields can be defined by [33]:

$$\begin{aligned} u(x,y,z,t)&=u_0(x,y,t)-z\frac{\partial w_b}{\partial x}+f(z)\frac{\partial w_s}{\partial x}\\ v(x,y,z,t)&=v_0(x,y,t)-z\frac{\partial w_b}{\partial y}+f(z)\frac{\partial w_s}{\partial y}\\ w(x,y,z,t)&=w_b(x,y,t)+w_s(x,y,t) \end{aligned} \tag{4}$$

In which $t$ represents the time, $u_0$ and $v_0$ signify the displacement functions of the middle surfaces of the deck plate. Also, $f(z)$ is the representative shape function that denotes the distribution of transverse shear stress or strain along the deck plate thickness. The representative shape function and its first derivative are illustrated in equation (5) below:

$$f(z)=\frac{5z}{4}\left(1-\frac{4z^2}{3h^2}\right) \quad \text{and} \quad g(z)=f'(z)=\frac{df(z)}{dz}=\frac{5}{4}-\frac{5z^2}{h^2} \tag{5}$$

The high order shear deformation theory (HSDT) takes into account transverse shear strain in its formulation with the following assumptions.

1) The displacements are small in comparison with the deck plate thickness, and, therefore, strains involved are infinitesimal.
2) The transverse displacement, w includes two components one of bending ($w_b$), and the other of shear ($w_s$). The bending and shear parts are functions of coordinates x, y and t only, and the stretching part is a function x, y, t and z.
3) The in-plane displacements ($u$ and $v$) in coordinates $x$ and $y$ are divided into extension, bending and shear parts. It is shown that the in-plane displacements are functions of $x$, $y$, $t$ and $z$ in which the bending parts are similar to those presented by classical plate theory (CPT), and shear parts of that are in conjunction with the hyperbolic variations of shear strains.

The strains associated with the displacements in Equation (4) are:

$$\begin{Bmatrix}\varepsilon_x\\ \varepsilon_y\\ \gamma_{xy}\end{Bmatrix}=\begin{Bmatrix}\varepsilon_x^0\\ \varepsilon_y^0\\ \gamma_{xy}^0\end{Bmatrix}+z\begin{Bmatrix}k_x^b\\ k_y^b\\ k_{xy}^b\end{Bmatrix}+f(z)\begin{Bmatrix}k_x^s\\ k_y^s\\ k_{xy}^s\end{Bmatrix},\begin{Bmatrix}\gamma_{yz}\\ \gamma_{xz}\end{Bmatrix}=g(z)\begin{Bmatrix}\gamma_{yz}^s\\ \gamma_{xz}^s\end{Bmatrix},\varepsilon_z=0 \tag{6}$$

$$\begin{Bmatrix}\varepsilon_x^0\\ \varepsilon_y^0\\ \gamma_{xy}^0\end{Bmatrix}=\begin{Bmatrix}\dfrac{\partial u_0}{\partial x}\\ \dfrac{\partial v_0}{\partial y}\\ \dfrac{\partial u_0}{\partial y}+\dfrac{\partial v_0}{\partial x}\end{Bmatrix},\begin{Bmatrix}k_x^b\\ k_y^b\\ k_{xy}^b\end{Bmatrix}=\begin{Bmatrix}-\dfrac{\partial^2 w_b}{\partial x^2}\\ -\dfrac{\partial^2 w_b}{\partial y^2}\\ -2\dfrac{\partial^2 w_b}{\partial x\partial y}\end{Bmatrix},\begin{Bmatrix}k_x^s\\ k_y^s\\ k_{xy}^s\end{Bmatrix}=\begin{Bmatrix}\dfrac{\partial^2 w_s}{\partial x^2}\\ \dfrac{\partial^2 w_s}{\partial y^2}\\ 2\dfrac{\partial^2 w_s}{\partial x\partial y}\end{Bmatrix},$$

$$\begin{Bmatrix}\gamma_{yz}^s\\ \gamma_{xz}^s\end{Bmatrix}=\begin{Bmatrix}\dfrac{\partial w_s}{\partial y}\\ \dfrac{\partial w_s}{\partial x}\end{Bmatrix}, \tag{7}$$

The stress-strain relations for an isotropic linear elastic plate, are written in the following equation:

$$\begin{Bmatrix}\sigma_x\\ \sigma_y\\ \tau_{xy}\end{Bmatrix}=\begin{bmatrix}Q_{11} & Q_{12} & 0\\ Q_{12} & Q_{22} & 0\\ 0 & 0 & Q_{66}\end{bmatrix}\begin{Bmatrix}\varepsilon_x\\ \varepsilon_y\\ \gamma_{xy}\end{Bmatrix}\begin{Bmatrix}\tau_{yz}\\ \tau_{zx}\end{Bmatrix}=\begin{bmatrix}Q_{44} & 0\\ 0 & Q_{55}\end{bmatrix}\begin{Bmatrix}\gamma_{yz}\\ \gamma_{zx}\end{Bmatrix} \tag{8}$$

where ($\sigma_x$ , $\sigma_y$ , $\tau_{xy}$ , $\tau_{yz}$ , $\tau_{yx}$) and ($\varepsilon_x$ , $\varepsilon_y$ , $\gamma_{xy}$ , $\gamma_{yz}$ , $\gamma_{yx}$) are the stress and strain components, respectively. Using the material properties defined in Equations (2a) and (3a), the stiffness coefficients, $Q_{ij,}$ can be expressed as in the following equation:

$$Q_{11}=Q_{22}=\frac{E(z)}{1-\nu^2},\quad Q_{12}=\frac{\nu\,E(z)}{1-\nu^2},\quad Q_{44}=Q_{55}=Q_{66}=\frac{E(z)}{2(1+\nu)}, \tag{9}$$

## 4 EQUATIONS OF MOTION

Hamilton's principle is used herein to derive the equations of motion. The principle can be stated in analytical from as stated in [34].

$$\int_0^T(\delta U-\delta K)dt=0 \tag{10}$$

Where $\delta U$: variation of strain energy; $\delta K$: variation of kinetic energy. The variation of strain energy of the plate is calculated by

$$\delta U = \int_{-h/2}^{h/2} \int_A \left[ \sigma_x \delta\, \varepsilon_x + \sigma_y \delta\, \varepsilon_y + \tau_{xy} \delta\, \gamma_{xy} + \tau_{yz} \delta\, \gamma_{yz} + \tau_{xz} \delta\, \gamma_{xz} \right] dA\, dz \quad (11a)$$

$$\begin{aligned} \delta U = \int_A \big[ & N_x \delta \varepsilon_x^0 + N_y \delta \varepsilon_y^0 + N_{xy} \delta \varepsilon_{xy}^0 + M_x^b \delta k_x^b + M_y^b \delta k_y^b + M_{xy}^b \delta k_{xy}^b \\ & + M_x^s \delta k_x^s + M_y^s \delta k_y^s + M_{xy}^s \delta k_{xy}^s + S_{yz}^s \delta \gamma_{yz}^s \\ & + S_{xz}^s \delta \gamma_{xz}^s \big] dA \end{aligned} \quad (11b)$$

Where, h/2 is the top surface, and stress resultants and couples N, M, and S are defined by.

$$\begin{Bmatrix} N_x, & N_y, & N_{xy} \\ M_x^b, & M_y^b, & M_{xy}^b \\ M_x^s, & M_y^s, & M_{xy}^s \end{Bmatrix} = \int_{-h/2}^{h/2} \left( \sigma_x, \sigma_y, \tau_{xy} \right) \begin{Bmatrix} 1 \\ z \\ f(z) \end{Bmatrix} dz,$$

$$\left( S_{xz}^s, S_{yz}^s \right) = \int_{-h/2}^{h/2} \left( \tau_{xz}, \tau_{yz} \right) g(z) dz. \quad (12)$$

The variation of kinetic energy of the deck plate can be written as in the following equation.

$$\delta K = \int_{-h/2}^{h/2} \int_A \rho Z (\ddot{u} \delta u + \ddot{v} \delta v + \ddot{w} \delta w) dA dZ \quad (13)$$

Where dot-superscript convention indicates the differentiation with respect to the time variable t; and ($I_1$, $I_2$, $I_3$, $I_4$, $I_5$, $I_6$) are mass inertias defined as shown in equation (14) below:

$$\left( I_1, I_2, I_3, I_4, I_5, I_6 \right) = \int_{-h/2}^{h/2} \left( 1, z, z^2, f(z), z f(z), f(z)^2 \right) \rho(z) dz \quad (14)$$

Substituting the expressions for $\delta U$ and $\delta K$ from Equations (11) and (13) into Equation (10), integrating the displacement gradients by parts and setting the coefficients $\delta u$, $\delta v$, $\delta w_b$, and $\delta w_s$ to zero separately. Thus, equilibrium equations associated with the present shear deformation theory could be obtained,

$$\delta u: \quad \frac{\partial N_x}{\partial x} + \frac{\partial N_{xy}}{\partial y} = I_1 \ddot{u}_o - I_2 \frac{\partial \ddot{w}_b}{\partial x} - I_4 \frac{\partial \ddot{w}_s}{\partial x}$$

$$\delta v: \quad \frac{\partial N_{xy}}{\partial x} + \frac{\partial N_y}{\partial y} = I_1 \ddot{v}_o - I_2 \frac{\partial \ddot{w}_b}{\partial y} - I_4 \frac{\partial \ddot{w}_s}{\partial y}$$

$$\delta w_b: \quad \frac{\partial^2 M_x^b}{\partial x^2} + 2\frac{\partial^2 M_{xy}^b}{\partial x \partial y} + \frac{\partial^2 M_y^b}{\partial y^2} = I_1(\ddot{w}_b + \ddot{w}_s) + I_2\left(\frac{\partial \ddot{u}}{\partial x} + \frac{\partial \ddot{v}}{\partial y}\right) - I_3\left(\frac{\partial^2 \ddot{w}_b}{\partial x^2} + \frac{\partial^2 \ddot{w}_b}{\partial y^2}\right) - I_5\left(\frac{\partial^2 \ddot{w}_s}{\partial x^2} + \frac{\partial^2 \ddot{w}_s}{\partial y^2}\right)$$

$$\delta w_s: \quad \frac{\partial^2 M_x^s}{\partial x^2} + 2\frac{\partial^2 M_{xy}^s}{\partial x \partial y} + \frac{\partial^2 M_y^s}{\partial y^2} + \frac{\partial S_{xz}^s}{\partial x} + \frac{\partial S_{yz}^s}{\partial y} = I_1(\ddot{w}_b + \ddot{w}_s) + I_4\left(\frac{\partial \ddot{u}}{\partial x} + \frac{\partial \ddot{v}}{\partial y}\right) - I_5\left(\frac{\partial^2 \ddot{w}_b}{\partial x^2} + \frac{\partial^2 \ddot{w}_b}{\partial y^2}\right) - I_6\left(\frac{\partial^2 \ddot{w}_s}{\partial x^2} + \frac{\partial^2 \ddot{w}_s}{\partial y^2}\right) \tag{15}$$

By substituting Equation (6) into Equation (8) and integrating through the thickness of the deck plate, the stress resultants are given as follows:

$$\begin{Bmatrix} N \\ M^b \\ M^s \end{Bmatrix} = \begin{bmatrix} A & B & B^s \\ A & D & D^s \\ B^s & D^s & H^s \end{bmatrix} \begin{Bmatrix} \varepsilon \\ k^b \\ k^s \end{Bmatrix}, \quad S = A^s \gamma \tag{16}$$

$$N = \left\{N_x, N_y, N_{xy}\right\}^t,\ M^b = \left\{M_x^b, M_y^b, M_{xy}^b\right\}^t,\ M^s = \left\{M_x^s, M_y^s, M_{xy}^s\right\}^t \tag{17a}$$

$$\varepsilon = \left\{\varepsilon_x^0, \varepsilon_y^0, \gamma_{xy}^0\right\}^t, k^b = \left\{k_x^b, k_y^b, k_{xy}^b\right\}^t, k^s = \left\{k_x^s, k_y^s, k_{xy}^s\right\}^t \tag{17b}$$

$$A = \begin{bmatrix} A_{11} & A_{12} & 0 \\ A_{12} & A_{22} & 0 \\ 0 & 0 & A_{66} \end{bmatrix}, B = \begin{bmatrix} B_{11} & B_{12} & 0 \\ B_{12} & B_{22} & 0 \\ 0 & 0 & B_{66} \end{bmatrix}, D = \begin{bmatrix} D_{11} & D_{12} & 0 \\ D_{12} & D_{22} & 0 \\ 0 & 0 & D_{66} \end{bmatrix} \tag{17c}$$

$$B^s = \begin{bmatrix} B_{11}^s & B_{12}^s & 0 \\ B_{12}^s & B_{22}^s & 0 \\ 0 & 0 & B_{66}^s \end{bmatrix}, D^s = \begin{bmatrix} D_{11}^s & D_{12}^s & 0 \\ D_{12}^s & D_{22}^s & 0 \\ 0 & 0 & D_{66}^s \end{bmatrix}, H^s = \begin{bmatrix} H_{11}^s & H_{12}^s & 0 \\ H_{12}^s & H_{22}^s & 0 \\ 0 & 0 & H_{66}^s \end{bmatrix} \tag{17d}$$

$$S = \left\{S_{xz}^s, S_{yz}^s\right\}^t, \gamma = \left\{\gamma_{xz}, \gamma_{yz}\right\}^t, A^s = \begin{bmatrix} A_{44}^s & 0 \\ 0 & A_{55}^s \end{bmatrix} \tag{17e}$$

Where $A_{ij}$, $B_{ij,}$ etc. are the deck plate stiffness defined by:

$$\left\{A_{ij},B_{ij},D_{ij}\right\}=\int_{-h/2}^{h/2}\left(1,z,z^2\right)Q_{ij}dz \qquad (i,j=1,2,6)$$

$$\left\{B_{ij}^s,D_{ij}^s,H_{ij}^s\right\}=\int_{-h/2}^{h/2}\left(f(z),z\,f(z),f^2(z)\right)Q_{ij}dz \qquad (i,j=1,2,6)$$

$$\left\{A_{ij}^s\right\}=\int_{-h/2}^{h/2}\left(\left[g(z)\right]^2\right)Q_{ij}dz, \qquad (i,j=4,5) \tag{18}$$

Rectangular deck plates are generally classified according to the type of support used. This research paper is concerned with the exact solution for a simply supported FG plate. The following boundary conditions are imposed at the side edges:

$$v_0=w_b=w_s=\frac{\partial w_b}{\partial y}=\frac{\partial w_s}{\partial y}=N_x=M_x^b=M_x^s=0 \quad and \quad x=0,\ a \tag{19a}$$

$$u_0=w_b=w_s=\frac{\partial w_b}{\partial x}=\frac{\partial w_s}{\partial x}=0, N_y=M_y^b=M_y^s=0 \quad and \quad y=0,\ b \tag{19b}$$

Following the Navier solution procedure, we assume the following form of solution for ($u$, $v$, $wb$, $ws$) that satisfies the boundary conditions given in Equation (19).

$$\begin{Bmatrix} u \\ v \\ w_b \\ w_s \end{Bmatrix}=\sum_{m=1}^{\infty}\sum_{n=1}^{\infty}\begin{Bmatrix} U_{mn}e^{i\omega t}\cos(\lambda x)\sin(\mu y) \\ V_{mn}e^{i\omega t}\sin(\lambda x)\cos(\mu y) \\ W_{bmn}e^{i\omega t}\sin(\lambda x)\sin(\mu y) \\ W_{smn}e^{i\omega t}\sin(\lambda x)\sin(\mu y) \end{Bmatrix}, \tag{20}$$

Where $\boldsymbol{\lambda=m\pi/a}$ and $\boldsymbol{\mu=n\pi/b}$, «$\boldsymbol{m}$» and «$\boldsymbol{n}$»are mode numbers and $U_{mn}$, $V_{mn}$, $W_{bmn}$, and $W_{smn}$ are arbitrary parameters. These parameters could be combined into a system of equations as shown in equation (21) below:

$$\left(\left[K\right]-\omega^2\left[M\right]\right)\{\Delta\}=\{0\}, \tag{21}$$

Where [K] and [M], stiffness and mass matrices, respectively, which are represented as:

$$\left(\begin{bmatrix} a_{11} & a_{12} & a_{13} & a_{14} \\ a_{12} & a_{22} & a_{23} & a_{24} \\ a_{13} & a_{23} & a_{33} & a_{34} \\ a_{14} & a_{24} & a_{34} & a_{44} \end{bmatrix}-\omega^2\begin{bmatrix} m_{11} & 0 & 0 & 0 \\ 0 & m_{22} & 0 & 0 \\ 0 & 0 & m_{33} & m_{34} \\ 0 & 0 & m_{34} & m_{44} \end{bmatrix}\right)\begin{Bmatrix} U_{mn} \\ V_{mn} \\ W_{bmn} \\ W_{smn} \end{Bmatrix}=\begin{Bmatrix} 0 \\ 0 \\ 0 \\ 0 \end{Bmatrix} \tag{22}$$

In which,

$$a_{11}=-(A_{11}\lambda^2+A_{66}\mu^2);\ a_{12}=-\lambda\mu(A_{12}+A_{66});\ a_{13}=\lambda(B_{11}\lambda^2+(B_{12}+2B_{66})\mu^2);$$

$$a_{14} = \lambda(B_{11}^s\lambda^2 + (B_{12}^s + 2B_{66}^s)\mu^2);\ a_{21} = a_{12};\ a_{22} = -(A_{66}\lambda^2 + A_{22}\mu^2);$$

$$a_{23} = \mu\big((B_{12} + 2B_{66})\lambda^2 + B_{22}\mu^2\big);\ a_{24} = \mu\big((B_{12}^s + 2B_{66}^s)\lambda^2 + B_{22}^s\mu^2\big);\ a_{31} = a_{13};\ a_{32} = a_{23;}$$

$$a_{33} = -(D_{11}\lambda^4) + 2(D_{12} + 2D_{66}\lambda^2\mu^2 + D_{22}\mu^4);\ a_{34} = -(D_{11}^s\lambda^4) + 2(D_{12}^s + 2D_{66}^s\lambda^2\mu^2 + D_{22}^s\mu^4);$$

$$a_{41} = a_{14};\ a_{42} = a_{24;}\ a_{31} = a_{13};\ a_{43} = a_{34;}\ a_{44} = -(H_{11}^s\lambda^4) + 2(H_{12}^s + 2H_{66}^s\lambda^2\mu^2 + H_{22}^s\mu^4 + A_{55}^s\lambda^2 + A_{44}^s\mu^2) \quad (23)$$

$$m_{11} = -I_1;\ m_{13} = \lambda I_2\ ;\ m_{14} = \lambda I_4;\quad m_{22} = -I_1\ ;\ m_{23} = \mu I_2\ ;\ m_{24} = \mu I_4 \quad (24)$$

## 5 NUMERICAL RESULTS AND DISCUSSIONS

In this section, some numerical examples are performed and discussed to demonstrate the effectiveness of the theory proposed in the responses of the free vibration of simply supported (FGM) deck plates. Based on the equations of the system and the solution procedure in previous section, the numerical results and detailed discussions are presented here. For numerical results, an $Al/Al_2O_3$ functionally graded plate (FGP) which is composed of Aluminum and Alumina is considered. The Young's modulus and density of Aluminum are $E_m$=70GPa and $\rho_m$=2702kg/m$^3$, and that of Alumina $E_m$=380GPa and $\rho_m$=3800kg/m$^3$, respectively. The non-dimensional entities were used as shown below:

$$\bar{\beta}=\omega h\sqrt{\rho_c / E_c}\ ,\quad \tilde{\beta}=\omega h\sqrt{\rho_m / E_m}\ ,\quad \bar{\omega}=\omega a^2 / h\sqrt{\rho_c / E_c} \quad (25)$$

Natural frequencies obtained from the present study are compared with those available in the literature for (FGP) plates in Table 1, the results are found completely coincident with the present approach.

In Table 2, four fundamental frequencies of simply supported rectangular deck plate (FGP) with two different porosity distributions Even and Uneven are compared with their counterpart in the literature of Rezaei et al [20] and Askari [21]. The results presented show a good agreement with the other results which confirm the accuracy of the current approach.

In Table 3, another comparison is made of the fundamental natural frequencies of a rectangular deck plate $Al/Al_2O_3$ (b=2a). The same behavior is observed. That is to say, there is an excellent agreement between the results given by this model and those of the literature used in the study. It should be noted that, for validation reasons, the results presented in the three tables are

obtained for a (FGM) plate. In the verification process, we could say that the present method is reliable for the study of the plates presenting manufacturing porosity defects.

*Table 1.* Comparison of fundamental frequency $\left(\bar{\beta}\right)$ for simply supported (FGP) and (a=b=1)

| h/a | Method | p | | |
|---|---|---|---|---|
| | | 0 | 1 | 4 |
| 0.05 | Benachour et al [16] | 0,0148 | 0,0113 | 0,0098 |
| | Belabed et al [17] | 0,0148 | 0,0113 | 0,0098 |
| | Rezaei et al [20] | 0,0148 | 0,0113 | 0,0098 |
| | **Present** | **0,0148** | **0,0113** | **0,0098** |
| 0.1 | Benachour et al [16] | 0,0576 | 0,0441 | 0,0380 |
| | Belabed et al [17] | 0,0578 | 0,0449 | 0,0389 |
| | Rezaei et al [20] | 0,0578 | 0,0442 | 0,0383 |
| | **Present** | **0,0577** | **0,0442** | **0,0381** |
| 0.2 | Benachour et al [16] | 0,2112 | 0,1628 | 0,1375 |
| | Belabed et al [17] | 0,2121 | 0,1640 | 0,1383 |
| | Rezaei et al [20] | 0,2127 | 0,1630 | 0,1405 |
| | **Present** | **0,2113** | **0,1631** | **0,1378** |

*Table 2.* Comparison of fundamental frequency $\left(\tilde{\beta}\right)$ for simply supported square (b=a=1) deck plate (FGP) (P=1 and h/a=0.05)

| **Porosity Distribution** | **ξ** | **Method** | **Mode (m,n)** | | | |
|---|---|---|---|---|---|---|
| | | | **(1, 1)** | **(1, 2)** | **(2, 2)** | **(1, 3)** |
| **(Even)** | **ξ=0.1** | Rezaei et al [20] | 0,0217 | 0,0538 | 0,0851 | 0,1057 |
| | | Askari et al [21] | 0,0217 | 0,0537 | 0,0850 | 0,1055 |
| | | Present | 0,0213 | 0,0527 | 0,0833 | 0,1034 |
| | **ξ=0.2** | Rezaei et al [20] | 0,0210 | 0,0520 | 0,0824 | 0,1024 |
| | | Askari et al [21] | 0,0210 | 0,0520 | 0,0823 | 0,1022 |
| | | Present | 0,0203 | 0,0502 | 0,0794 | 0,0985 |
| **(Uneven)** | **ξ=0.1** | Rezaei et al [20] | 0,0224 | 0,0553 | 0,0874 | 0,1085 |
| | | Askari et al [21] | 0,0223 | 0,0552 | 0,0873 | 0,1083 |
| | | Present | 0,0208 | 0,0514 | 0,0814 | 0,1010 |
| | **ξ=0.2** | Rezaei et al [20] | 0,0225 | 0,0555 | 0,0879 | 0,1091 |
| | | Askari et al [21] | 0,0224 | 0,0554 | 0,0877 | 0,1087 |
| | | Present | 0,0191 | 0,0472 | 0,0747 | 0,0927 |

*Table 3.* Comparison of natural frequencies ($\bar{\omega}$) a rectangular deck plate $Al/Al_2O_3$

| a/h | Model | P=1 | | |
|---|---|---|---|---|
| | | **ξ=0** | **ξ=0.1** | **ξ=0.2** |
| 5 | Mouaici et al [31] | 2,6476 | 2,5934 | 2,5150 |
| | Present | 2,64753 | 2,54205 | 2,42474 |
| 10 | Mouaici et al [32] | 2,7937 | 2,7328 | 2,6452 |
| | Present | 2,79367 | 2,68017 | 2,55388 |

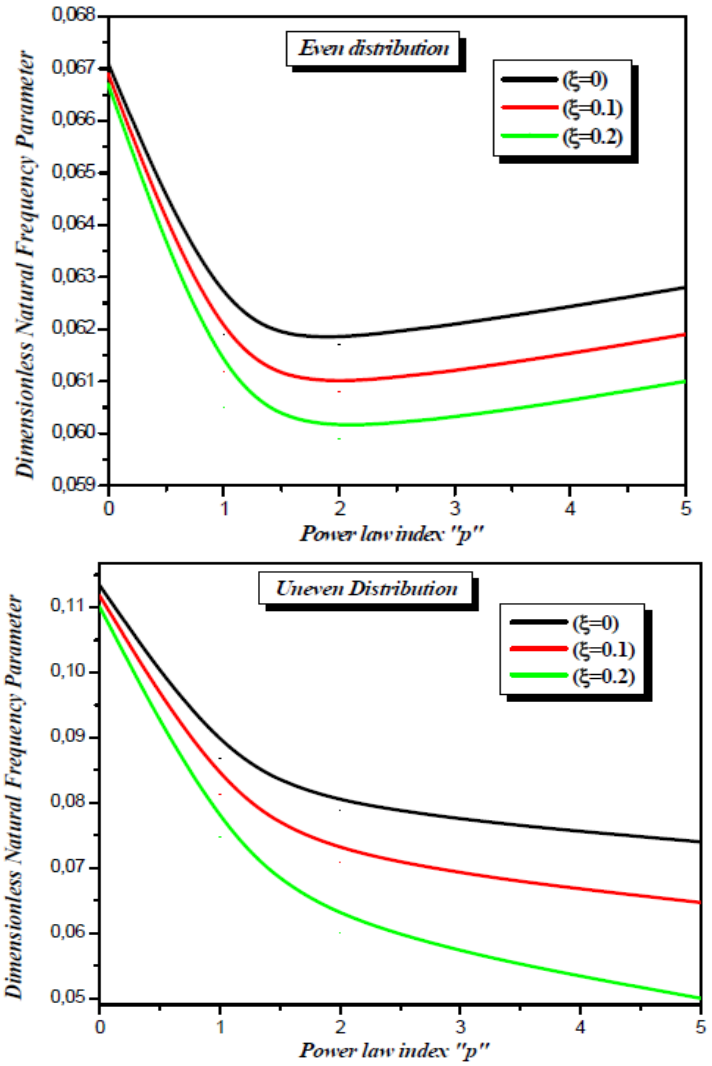


*Figure 3.* Dimensionless natural frequency parameter of the (FGM) plates according to the material power index “P” and porosity factor, (mode1, a=b and a/h=10)

As the material power index increases for (FGM) plates, the dimensionless natural frequency will decrease. The variation curves of the natural frequency of the first mode of various functionally graded plates, perfect and imperfect and for the two distributions of porosity even and uneven as a function of material power index parameter ‘’P’’, and for different values of porosity factor were presented in Figure 3. It can be seen that the increase of porosity parameter leads to an increase of the natural frequency for the first mode.

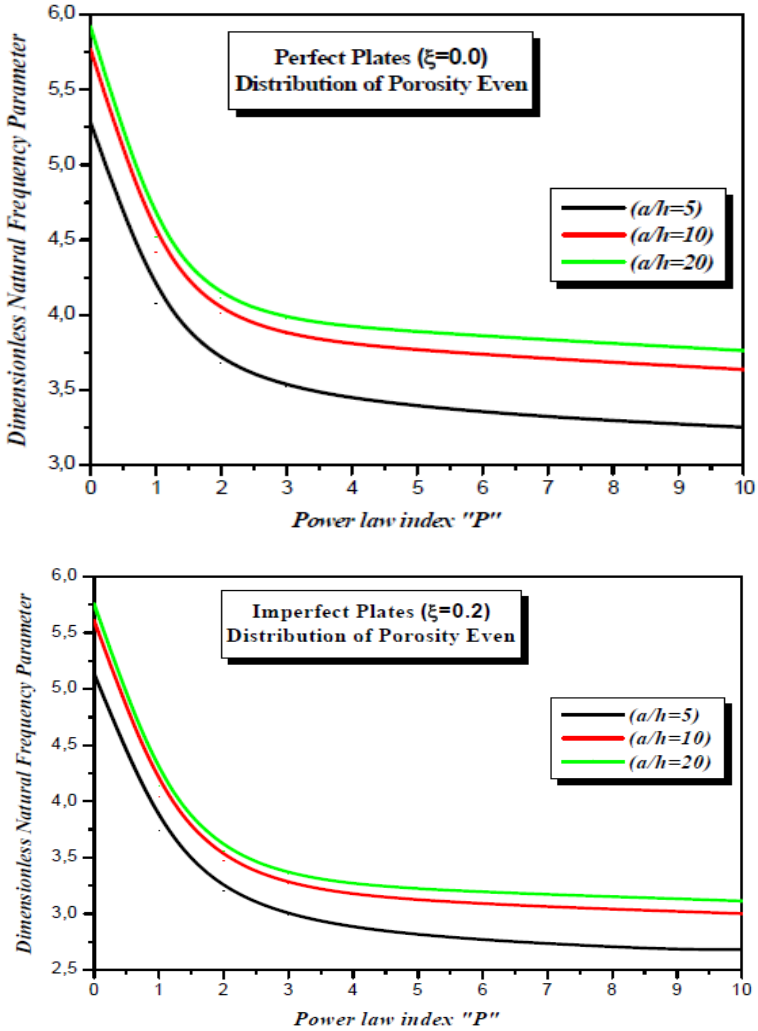


*Figure 4.* Influence of thickness ratio (a/h) on the dimensionless natural frequency parameter ($\bar{\omega}$) of the perfect and imperfect plate (FGM) for even distribution of porosity

Figure 4 shows the influence of thickness ratio (a/h), on the dimensionless natural frequency parameter of (FGM) perfect plates (ξ=0) and imperfect plates (ξ = 0.2) for the even distribution of porosity. It can be seen that the increase in thickness ratio (a/h) decreases the natural frequency. This conclusion implies that thickness ratio has a considerable effect on the natural frequency.

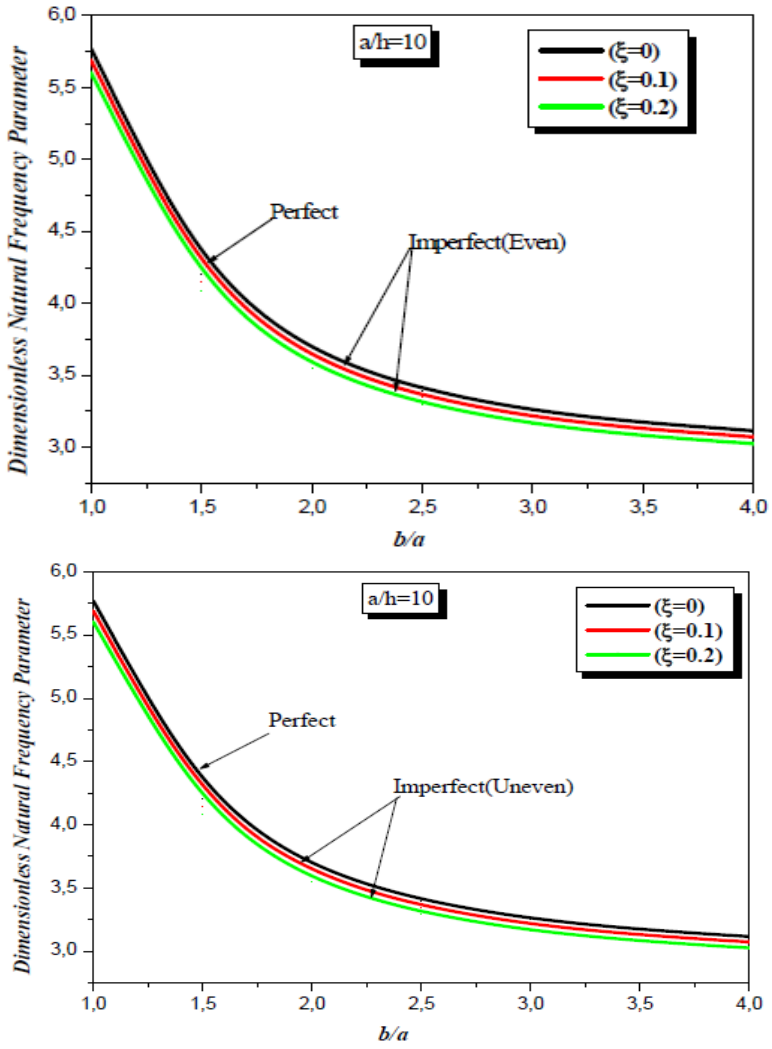


*Figure 5.* Dimensionless natural frequency ( $\overline{\omega}$ ) as a function of the geometric ratio (b/a) for the two distributions of porosity (even and uneven)

Figure 5 studies the variation of the dimensionless natural frequency with the thickness ratio as a function of the geometric ratio (b/a) for the two distributions

of the porosity (Even and Uneven). Decreasing in geometric ratio increases the dimensionless natural frequency. Although the increase of the ratio (b/a) reduces the dimensionless natural frequency, it is noticed that the ratio (b/a) has little influence on the variation of the natural frequency. For geometric ratios (b/a≥3), the geometric ratio has practically no effect on the natural frequencies and this includes the two distributions of the porosity (Even and Uneven).

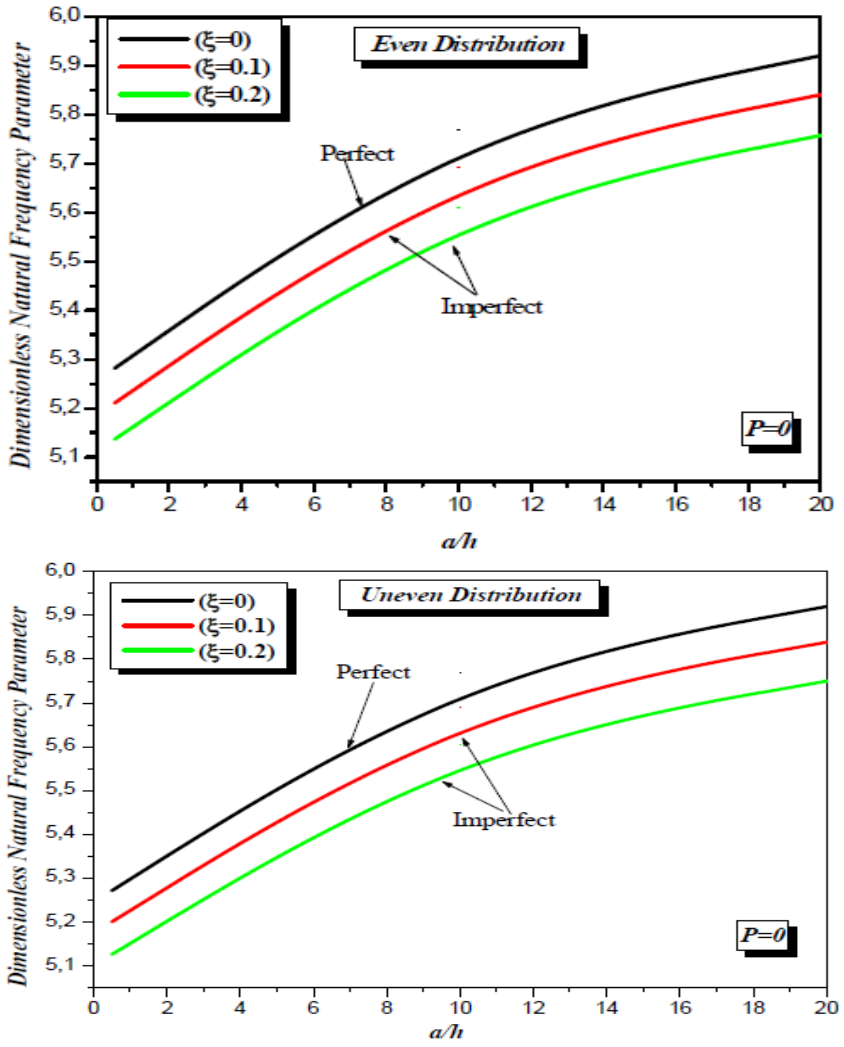


*Figure 6.* Variation of the dimensionless natural frequency ( $\overline{\omega}$ ) as a function of the thickness ratio (a/h) for the two distributions of porosity (even and uneven).

In Figure 6, the variation of the dimensionless natural frequency as a function of the thickness ratio (a/h) for the two distributions of the porosity (Even and

Uneven) is presented. There is a rapid variation in the frequency for the low values of the ratio (a/h) (i.e. for a / h <10) where the deck plate is considered thick. Exceeding this ratio, the dimensionless natural frequencies keep a more or less constant pace whatever the chosen distribution. In addition, it should be noted that the even distribution porosity gives higher values relative to the uneven porosity.

## 6 CONCLUSIONS

In this research article, an analytical study has been developed for free vibration analysis of square and rectangular porous functionally graded plate (FGP). In this investigation, the (FGM) plate is assumed to have two distribution of porosity Even and Uneven according to the thickness of the deck plate. The theory of shear deformations is used solve the equations of motion of the Hamiltonian principle. The accuracy of this theory is verified by comparing the developed results with those obtained using different numerical and analytical techniques and plate theories. Some examples are performed to demonstrate the effect of power index, porosity factor, length to thickness ratios and geometric ratios on the natural frequency of functionally graded plate (FGP). It has been demonstrated that the present analytical formulation method can accurately predict natural frequencies of (FGP) plates with porosity (Even and Uneven). Also, it can be concluded that the effect of volume fraction distributions, slenderness ratio and porosity on the dimensionless natural frequency is significant.

## REFERENCES

[1] Koizumi, M., FGM activities in Japan, Compos Part B, 28, pp. 1–4, (1997).
[2] Akbaş, Ş. D. Wave propagation of a functionally graded beam in thermal environments, Steel and Composite Structures, 19(6), pp. 1421-1447, (2015).
[3] Bennai, R., Ait Atmane, H., Tounsi, A. A new higher-order shear and normal deformation theory for functionally graded sandwich beams, Steel and Composite Structures, 19(3), pp. 521 – 546, (2015).
[4] Arefi, M. Elastic solution of a curved beam made of functionally graded materials with different cross sections, Steel and Composite Structures, 18(3), pp. 659 – 672, (2015).
[5] Ait Atmane, H., Tounsi, A., Bernard, F., Mahmoud, S.R. A computational shear displacement model for vibrational analysis of functionally graded beams with porosities, Steel and Composite Structures, 19(2), pp. 369-384, (2015).
[6] Ebrahimi, F., Dashti, S. Free vibration analysis of a rotating non-uniform functionally graded beam, Steel and Composite Structures, 19(5), pp. 1279 – 1298, (2015).
[7] Darılmaz, K., Vibration analysis of functionally graded material (FGM) grid systems, Steel and Composite Structures, 18(2), pp. 395 – 408, (2015).
[8] Ebrahimi, F., Habibi, S. Deflection and vibration analysis of higher-order shear deformable compositionally graded porous plate, Steel and Composite Structures, 20(1), pp. 205 - 225, (2016).
[9] Kar, V.R., Panda, S.K. Nonlinear thermomechanical deformation behavior of P-FGM shallow spherical shell panel, Chinese Journal of Aeronautics, 29(1), pp. 173 – 183, (2016).
[10] Moradi-Dastjerdi, R. Wave propagation in functionally graded composite cylinders

reinforced by aggregated carbon nanotube, Structural Engineering and Mechanics, 57(3), pp. 441 – 456, (2016).
[11] Trinh, T.H., Nguyen, D.K., Gan, B.S., Alexandrov, S. Post-buckling responses of elastoplastic FGM beams on nonlinear elastic foundation, Structural Engineering and Mechanics, 58(3), pp. 515 – 532, (2016).
[12] A. Hadj Mostefa, S. Merdaci, and N. Mahmoudi "An Overview of Functionally Graded Materials «FGM»", Proceedings of the Third International Symposium on Materials and Sustainable Development, ISBN 978-3-319-89706-6, pp. 267–278, (2018).
[13] Vel SS, Batra RC. Three-dimensional exact solution for the vibration of functionally graded rectangular plates. J Sound Vib; 272:703–30, (2004).
[14] Ferreira AJM, Batra RC, Roque CMC, Qian LF, Jorge RMN. Natural frequencies of functionally graded plates by a meshless method. Compos Struct; 75:593–600, (2006).
[15] Qian LF, Batra RC, Chen LM. Static and dynamic deformations of thick functionally graded elastic plates by using higher-order shear and normal deformable plate theory and meshless local Petrov–Galerkin method. Composites: Part B; 35:685–97, (2004).
[16] Benachour, A., Tahar, H. D., Atmane, H. A., Tounsi, A., Ahmed, M. S., A four variable refined plate theory for free vibrations of functionally graded plates with arbitrary gradient. Composites Part B: Engineering, 42(6), pp.1386-1394, (2011).
[17] Belabed, Z., Houari, M. S. A., Tounsi, A., Mahmoud, S. R., Bég, O. A., An efficient and simple higher order shear and normal deformation theory for functionally graded material (FGM) plates, Composites Part B: Engineering,60, pp.274-283, (2014).
[18] Uymaz B, Aydogdu M. Three-dimensional vibration analyses of functionally graded plates under various boundary conditions. J Reinforced Plates Compos; 26(18):1847–63, (2007).
[19] Matsunaga H. Free vibration and stability of functionally graded plates according to a 2-D higher-order deformation theory. Compos Struct; 82:499–512, (2008).
[20] Rezaei, A.S., Saidi, A.R., Application of Carrera Unified Formulation to study the effect of porosity on natural frequencies of thick porous-cellular plates, Composites Part B: Engineering, 91, pp. 361-70, (2016).
[21] Askari, Saidi A.R, Rezaei, A.S, Badizi.M.A, "Navier-type Free Vibration Analysis of Porous Smart Plates According to Reddy's Plate Theory" international conference on mechanics of advanced materials and equipment, (2018).
[22] Rezaei, A.S., Saidi,A.R.,On the effect of coupled solid-fluid deformation on natural frequencies of fluid saturated porous plates, European Journal of Mechanics-A/Solids,63, pp.99-109, (2017).
[23] Kamranfard, M.R., Saidi, A.R., Naderi, A., Analytical solution for vibration and buckling of annular sectorial porous plates under in-plane uniform compressive loading, Proceedings of the Institution of Mechanical Engineers, Part C: Journal of Mechanical Engineering Science, (2017).
[24] Merdaci, Hadj Mostefa A, "Influence of porosity on the analysis of sandwich plates FGM using of high order shear-deformation theory", Fracture ed Integrità Strutturale, 51, 199-214, (2020).
[25] Zhu, J., Lai, Z., Yin, Z., Jeon, J. and Lee, S. Fabrication of ZrO2–NiCr functionally graded material by powder metallurgy, Mater. Chem. Phys., 68(1), pp. 130-135, (2001).
[26] Wattanasakulpong, N. Prusty, B.G. Kelly, D.W. and Hoffman, M. Free vibration analysis of layered functionally graded beams with experimental validation. Mater. Des, 36, 182-190, (2012).
[27] Wattanasakulpong, N. and Ungbhakorn, V. Linear and nonlinear vibration analysis of elastically restrained ends FGM beams with porosities. Aerosp.Sci. Technol, 32(1), 111-120, (2014).
[28] Merdaci S, "Analysis of Bending of Ceramic-Metal Functionally Graded Plates with Porosities Using of High Order Shear Theory"; Advanced Engineering Forum; Vol.30, pp 54-70, (2018).

[29] Merdaci S, Belghoul.H, “High Order Shear Theory for Static Analysis Functionally Graded Plates with Porosities”, Comptes rendus Mecanique, Vol 347, Issue3, pp 207-217, (2019).
[30] Merdaci S, Belmahi S, Belghoul.H .H, Hadj Mostefa A, “Free Vibration Analysis of Functionally Graded Plates FG with Porosities”, International Journal of Engineering Research & Technology (IJERT), Vol. 8 Issue 03, pp143-147, (2019).
[31] Merdaci S, “Free Vibration Analysis of Composite Material Plates "Case of a Typical Functionally Graded FG Plates Ceramic/Metal" with Porosities”, Nano Hybrids and Composites (NHC), Vol. 25, pp 69-83, (2019).
[32] Mouaici F., Benyoucef S., Ait Atmane H., and Tounsi A., Effect of porosity on vibrational characteristics of non-homogeneous plates using hyperbolic shear deformation theory, Wind and Structures, 22 (4) ,429-454, (2016).
[33] S. Merdaci, A. Tounsi, M.S.A. Houari, I. Mechab, H. Hebali, S. Benyoucef, “Two new refined shear displacement models for functionally graded sandwich plates”, Arch. Appl. Mech. 81, 1507-1522, (2011).
[34] Reddy, J.N. Energy principles and variational methods in applied mechanics, Wiley, New York, (2002).